Journal of Asian Earth Sciences 148 (2017) 173–180

Contents lists available at ScienceDirect

Journal of Asian Earth Sciences

journal homepage: www.elsevier.com/locate/jseaes

Full length article

Preliminary observations from the 3 January 2017, M_W 5.6 Manu, Tripura (India) earthquake

Jimmi Debbarma[a], Stacey S. Martin[b], G. Suresh[c], Aktarul Ahsan[d], Vineet K. Gahalaut[c,*]

[a] Department of Geography and Disaster Management, Tripura University, Agartala, India
[b] Earth Observatory of Singapore, Nanyang Technological University, Singapore
[c] National Centre for Seismology, Ministry of Earth Sciences, New Delhi, India
[d] Geological Survey of Bangladesh, Dhaka, Bangladesh

ARTICLE INFO

Keywords:
Indo-Burmese arc
Tripura earthquake
Soil liquefaction
Intra-slab earthquake

ABSTRACT

On 3 January 2017, a M_W 5.6 earthquake occurred in Dhalai district in Tripura (India), at 14:39:03 IST (09:09:03 UTC) with an epicentre at 24.018°N ± 4.9 km and 91.964°E ± 4.4 km, and a focal depth of 31 ± 6.0 km. The focal mechanism solution determined after evaluating data from seismological observatories in India indicated a predominantly strike-slip motion on a steeply dipping plane. The estimated focal depth and focal mechanism solution places this earthquake in the Indian plate that lies beneath the overlying Indo-Burmese wedge. As in the 2016 Manipur earthquake, a strong motion record from Shillong, India, appears to suggest site amplification possibly due to topographic effects. In the epicentral region in Tripura, damage assessed from a field survey and from media reports indicated that the macroseismic intensity approached 6–7 EMS with damage also reported in adjacent parts of Bangladesh. A striking feature of this earthquake were the numerous reports of liquefaction that were forthcoming from fluvial locales in the epicentral region in Tripura, and at anomalous distances farther north in Bangladesh. The occurrence of the 2017 Manu earthquake emphasises the hazard posed by intraplate earthquakes in Tripura and in the neighbouring Bengal basin region where records of past earthquakes are scanty or vague, and where the presence of unconsolidated deltaic sediments and poor implementation of building codes pose a significant societal and economic threat during larger earthquakes in the future.

1. Introduction

The state of Tripura in north-eastern India is located within the Indo-Burmese wedge where crustal deformation and associated seismicity occur in response to the interaction of the Indian and Sunda plates (Le Dain et al., 1984; Guzman-Speziale et al., 1989; Guzman-Speciale and Ni, 1996). Tectonic features in this area were discussed by Le Dain et al. (1984), Maurin and Rangin (2009), Gahalaut et al. (2013) and Wang et al. (2014). The geodetically determined motion of ≈36 mm/year between the two plates (Socquet et al., 2006) is partitioned by slip along the Churachandpur Mao Fault (CMF) in the Indo-Burmese wedge (Gahalaut et al., 2013), and by motion on the Sagaing Fault (Vigny et al., 2003; Maurin et al., 2010) in Myanmar (Fig. 1). Earthquakes on the Sagaing Fault have shallow foci with predominantly strike-slip focal mechanisms on steep planes (Le Dain et al., 1984; Guzman-Speziale et al., 1989; Guzman-Speciale and Ni, 1996, Maurin et al., 2010). In the Indo-Burmese wedge region, the majority of earthquakes occur on steep planes within the Indian plate that lies below the Indo Burmese wedge (Rao and Kalpna, 2005; Kundu and Gahalaut, 2012; Russo, 2012; Gahalaut and Kundu, 2016). An important implication of the latter is the status of the dipping décollement surface between the overriding Indo-Burmese wedge and the underlying Indian lithospheric slab. Using a model supported by geodetic measurements from India and Myanmar, Gahalaut et al. (2013) suggested that the motion between the Indian and the Burma plate in the wedge occurs primarily on the Churachandpur-Mao fault that separates the outer wedge to the west from the inner wedge and its core to the east, and that this structure is a splay from an eastward extending décollement. Steckler et al. (2016) supplemented data from India and Myanmar with geodetic observations from Bangladesh to propose an alternative model that suggests the décollement surface under the outer wedge is also seismically active, and accommodates strain that could be released in future interface rupturing earthquakes. We note that the 2017 Manu, Tripura earthquake occurred beneath the outer wedge of the Indo-Burmese arc, which has an apparently lower seismic moment release during the historical and instrumental eras in contrast to adjacent regions. Therefore the preliminary analysis of observations from the 2017 Manu, Tripura earthquake presented in this article offer a

* Corresponding author.
E-mail address: vkgahalaut@yahoo.com (V.K. Gahalaut).

http://dx.doi.org/10.1016/j.jseaes.2017.08.030
Received 16 February 2017; Received in revised form 20 August 2017; Accepted 25 August 2017
Available online 01 September 2017
1367-9120/

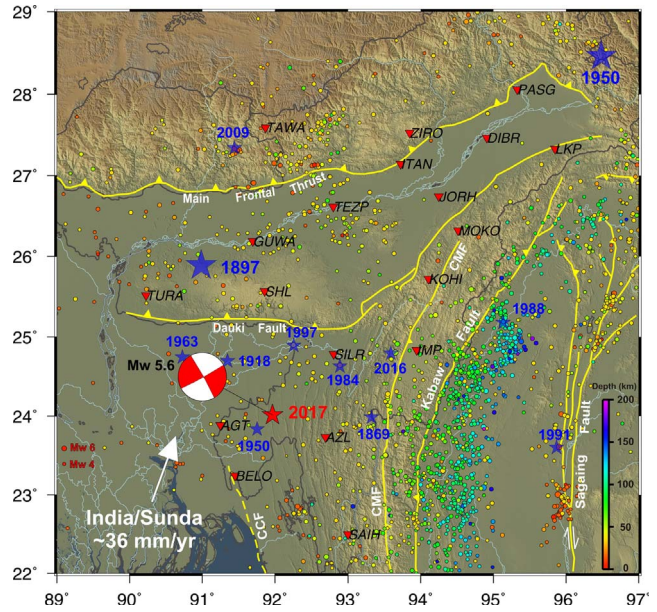

Fig. 1. Regional tectonics, seismological stations (red inverted triangles), along with earthquakes from 1973 to 2016 (ISC and USGS). CCF- Chittagong Coastal Fault, CMF- Churachandpur Mao Fault. A beachball representation of the 2017 Manu earthquake using parameters determined in this study is also shown. Stars represent events discussed in the text, or regionally significant earthquakes. The 1897 Shillong Plateau and 1950 Assam earthquakes are also shown. (For interpretation of the references to color in this figure legend, the reader is referred to the web version of this article.)

crucial opportunity to contribute to the ongoing efforts (e.g. Ahsan et al., 2015) to understand the seismic hazard potential of a region that lies in close proximity to the densely populated Ganga-Brahmaputra basin, vulnerable to amplification of ground motion in unconsolidated, or reworked deltaic sediments (e.g. Islam et al., 2010; Asad et al., 2015; Khan, 2015).

2. Seismicity of Tripura

The 2017 Manu, Tripura earthquake is one of the strongest instrumentally recorded earthquakes within the state borders of Tripura in at least half a century. Prior to 2017, the largest known earthquake occurred on 29 December 1950 with a local magnitude (M_L) of 6.3 which was located by Tandon (1954) in the central Balisera Valley (24.39°N, 91.74°E) (Fig. 1). The location and magnitude of this event were revised by Storchak et al. (2013) who relocated it in central Tripura (23.85°N, 91.84°E) and calculated M_W 5.9 ± 0.26. We did not find additional information for this earthquake. Sohoni (1951) reports it was felt at Aizawl (23.72°N, 92.71°E), Karimganj (24.86°N, 92.34°E) and Silchar (24.83°N, 92.77°E).

In the 19th century, the Cachar earthquake on 10 January 1869 caused heavy damage in the Silchar area of lower Assam (Oldham, 1883a) but its effects in Tripura are unknown. The 12 June 1897 Shillong earthquake, on the other hand, severely damaged the Maharaja's palace (*Friend of India*, 22–29 June 1897) and destroyed many buildings and shrines in Agartala (Hunter et al., 1909). It also raised the beds of many rivers notably that of the Manu (Hunter et al., 1909). The most significant earthquake in the immediate vicinity of the 2017 Manu earthquake during this period is the 8 July 1918 Sreemangal (also Srimangal or Srimongal) earthquake in the Balisera Valley with a moment magnitude (M_W) 7.4 (Pacheco and Sykes, 1992) and an intensity magnitude (M_I) between 6.8 and 7.1 (Ambraseys and Douglas, 2004; Szeliga et al., 2010). Within the Balisera Valley, severe shaking rendered it difficult to stand and people were thrown to the ground (Stuart, 1919, 1920). Single-storied, steel framed buildings with masonry infill walls suffered Grade 4 or greater damage, effects determined to be approximately equivalent to 8 EMS by Martin and Szeliga (2010). Hilly and forested tracts in Tripura, and regions of Sylhet flooded at the time, were not surveyed (Stuart, 1919) leaving the southern and northern extents of the meizoseismal zone poorly defined. However, in Agartala sand blows occurred and cracks were observed in roads (*Englishman*, 15 July 1918, repeated in Stuart, 1920). The upper storey of the Kunjabon Palace was badly damaged and had to be dismantled, and four domes of the Lakshminarayan temple collapsed (*Englishman*, 15 July 1918). Regionally, damage and fatalities occurred as far as Dhaka where, among other structures, the walls and *chhattris* of the Hossaini Dalan mosque needed repair or reconstruction (Anonymous, 1920). Varying grades of building damage also occurred in the large urban centres of Chittagong, Jamalpur, Mymensingh, Kolkata and Shillong (*Englishman*, 9–12 July 1918). As many as 53 fatalities were recorded in Sylhet district (Anonymous, 1919). Liquefaction features were reported from numerous locations within the mapped meizoseismal area as well as in Sylhet division (Stuart, 1920).

We would also like to draw attention to two earthquakes on 19 June 1963 and 21 June 1963 (M_W 5.6 ± 0.2 and M_W 5.7 ± 0.2 respectively) that were instrumentally located in Mymensingh division, Bangladesh (Storchak et al., 2013). Focal mechanisms for both earthquakes were computed and discussed by Chen and Molnar (1990). However, Modified Mercalli Intensities (MMI) reported by Tandon (1963), and repeated by Rothé (1969, p.188) for both earthquakes, appear to indicate that the highest intensities (MMI VII) were reported from further south at Kailashahar (24.32°N, 92.00°E) in Tripura, more than 60 km from the instrumented locations. Shaking from both earthquakes was widely perceived in Assam and Bengal: the first earthquake was felt as far as Bagdogra (26.69°N, 88.31°E) and Jorhat (26.74°N, 94.21°E). Although we rely on MMI assignments made by Tandon (1963) because first-hand accounts were unavailable to us, the spatial distribution of intensities, particularly for the 19 June 1963 earthquake, appear to suggest they both produced significantly higher ground motions away from their instrumentally determined epicentral locations, or more plausibly, that they were located closer to the region of the 2017 Manu earthquake.

3. Instrumental parameters

The 2017 Manu earthquake is one of the largest well instrumented earthquakes in the state of Tripura, since the establishment of the worldwide network of standardised seismographic stations (WWSSN) in the 1960s (Oliver and Murphy, 1971). It was well recorded by the broadband seismograph network operated by the National Centre for Seismology (NCS). The NCS has 84 seismological observatories that are part of the Indian national network connected to a central recording station at NCS in Delhi through VSAT. For the 2017 Manu earthquake, automatic preliminary earthquake parameters were determined within three minutes of the earthquake. We subsequently re-analysed the data from the closest 16 seismological stations (< 500 km) in north-eastern India, and more than 50 stations in the rest of the country. This allowed us to refine the epicentral location to 24.018°N ± 4.9 km and 91.964°E ± 4.4 km (Fig. 1) with a focal depth of 31 ± 6 km. Our estimate of the hypocentral depth was also constrained by sPn-Pn observations at nearby stations.

The seismic moment (M_o) of the earthquake is estimated to be 3.0×10^{24} dyne cm which corresponds to M_W 5.6 (Fig. 2). The estimated stress drop for the event is 20 MPa which is in the range of stress drops determined for other earthquakes in the immediate region (Allmann and Shearer, 2009; Raghukanth and Somala, 2009). Two aftershocks of magnitude (mb) 3.4 and 3.9 that occurred at 13:40:32 UTC on 4 January and at 15:03:52 UTC on 6 January respectively were also recorded by the national network. The parameters determined for the mainshock using data available to us from Indian observatories, show good correspondence with similar parameters determined by the United States Geological Survey (USGS), the European-Mediterranean

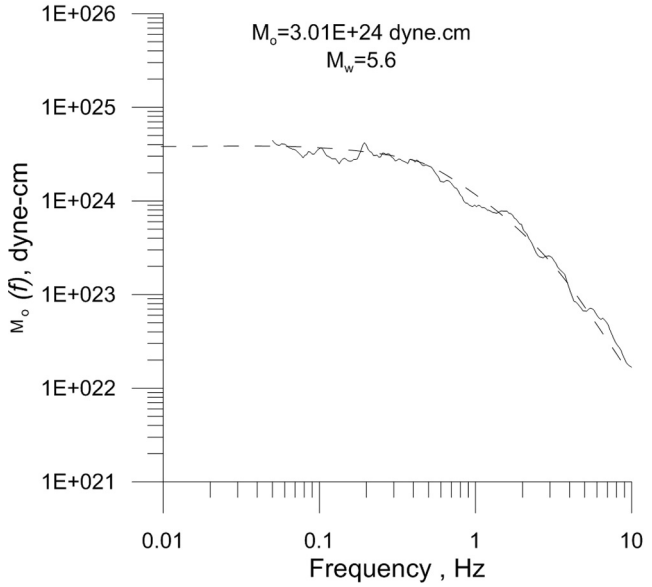

Fig. 2. Source displacement spectra of the earthquake, following Brune's (1970) ω^2 model. The obtained displacement spectra is the average of spectra at sites AGT, BELO, SHL, IMP, MOKO, ITA, TAWA, and BOKR.

Table 1
Comparison of source parameters for the Manu earthquake by various agencies.

Earthquake parameters	NCS	USGS	EMSC	Geophone
Origin time (UTC)	09:09:02	09:09:02	09:09:02.2.2	09:09:02.8
Epicentre	24.018°N, 91.964°E	24.016°N, 92.006°E	24.04°N, 92.03°E	24.01°N, 91.96°E
Focal depth (km)	31 ± 6	36.2	35 (fixed)	36
Magnitude (M_W)	5.6	5.5	5.6	5.6
Focal mechanism (strike, dip, rake)	331, 87, 177; 61, 87, 7	252, 89, 0; 162, 90, 179	–	337, 89, −174; 247, 85, 0

Seismological Centre (EMSC), and Geophone (Table 1). Due to its relatively low magnitude (M_W 5.6) and greater depth (31 km), this earthquake did not produce any coseismic offsets at nearby continuous GPS sites (e.g., Agartala).

The earthquake was also recorded by six strong motion accelerographs within 300 km of the epicentre, and at one station (Bokaro, BKRR) in eastern India at a distance of ≈620 km (Table 2). The highest peak ground acceleration (PGA) of 0.052 g (50.6 cm/s^2) was recorded by the instrument at Agartala (AGT) located ≈70 km from the epicentre. Interestingly, the instrument at Shillong (SHL) at a distance of ≈170 km recorded a PGA of 0.043 g (42.2 cm/s^2) on the north–south component. This value is higher than at other sites closer to the epicentre such as Belonia (0.026 g; 25.8 cm/s^2). Ground motion to intensity conversion equations (GMICE) have been derived for the United States and Canada using recorded ground motion parameters and observed macroseismic intensities (e.g. Wald et al., 1999; Atkinson, 2007; Worden et al., 2012). Hough et al. (2016) tested and verified the validity of the Worden et al. (2012) GMICE for use in the Indian subcontinent using macroseismic observations (Martin et al., 2015) and strong motions data from Nepal (Dixit et al., 2015) and India (Hough et al., 2016) for the Gorkha earthquake. We therefore use Worden et al. (2012) to convert the instrumental value at Shillong and obtain EMS_{PGA} 4.4, which is close to the observed intensity of 4–5 EMS.

Table 2
Peak ground acceleration from strong motion accelerographs.

Station name (station code)	Site condition and class	Latitude °N, Longitude °E	Epicentral distance, km	Peak ground acceleration, cm/s^2		
				Z	N-S	E-W
Agartala (AGT)	Stiff alluvial soil, D	23.889, 91.246	74	6.52	50.6	30.2
Belonia (BELO)	Stiff alluviul soil, D	23.248, 91.447	100	–	20.6	25.8
Shillong (SHL)	Hard rock, A	25.567, 91.856	172	11.7	42.2	35.5
Tura (TURA)	Hard rock, A	25.517, 90.224	242	7.93	10.3	13.8
Tezpur (TEZP)	Hard rock, A	26.617, 92.800	300	1.04	2.88	2.81
Bokaro (BOKR)	Rock, B	23.795, 85.886	619	0.13	0.31	0.18

Our focal mechanism solution, obtained from earthquake waveforms inversion based on the ISOLated Asperities (ISOLA) MT inversion code and SeisComP3 real-time processing system (Triantafyllis et al., 2015), shows a predominantly strike slip solution with either dextral motion on the NNW-SSE oriented vertical plane, or sinistral motion on the ENE-WSW oriented vertical plane (Fig. 1). This is consistent with the prevalent stress regime (Kundu and Gahalaut, 2012) in the Indo-Burmese wedge region and the relative India-Sunda plate motion (Socquet et al., 2006). The high PGA recorded at Shillong could be the result of directivity along strike (e.g. Benetatos and Kiratzi, 2004), and the strike of the highest macroseismic intensities (*following section*) probably hint at slip on the NNW-SSE oriented plane.

4. Macroseismic survey observations

We conducted a field survey from 4 to 6 January 2017 in the districts of Unakoti and Dhalai in Tripura, India. These field observations were supplemented by reports that appeared in local newspapers in India and Bangladesh. Our intensity data set for the 2017 Manu earthquake (Fig. 3; Table S1 in supplementary material) contains 114 locations of which 103 locations had both reliable geographic co-ordinates, carried information that was sufficient to assess numeric EMS-98 intensities, document where the earthquake was felt, or reported the occurrence of liquefaction.

We use the 1998 European Macroseismic Scale (EMS-1998; Grünthal, 1998) to maintain heterogeneity with previous studies (e.g. Martin and Szeliga, 2010). Although exceptions exist (e.g. Van Noten et al., 2016), the Modified Mercalli Scale (MMI) continues to dominate macroseismic studies both in India, and around the world (e.g. Du et al., 2016; Prajapati et al., 2017), in part owing to the most commonly used GMPE's (e.g. Atkinson, 2007) or GMICE (Worden et al., 2012) derived using extant MMI data from earthquakes in California, or the central and eastern United States (CEUS). Both the EMS-98 and the MMI scales were prepared with European societal and building conditions in mind, but the extensive guidelines (Grünthal, 1998) laid out for the EMS-98 scale provide greater flexibility for users to adapt it to non-European indigenous conditions and building types. Therefore, despite the misleading nature of the word "European" in its name, the EMS-98 scale, as was the case with its predecessor the MSK-64 scale, has enabled greater accuracy in intensity assignments in the Indian subcontinent as discussed by Martin and Hough (2016), and previously implemented by Martin and Kakar (2012), Martin and Hough, 2016, and Martin et al. (2015). The EMS-98 is generally consistent with the Modified Mercalli Scale (Musson et al., 2010). However, we follow the recommendation of Ambraseys and Melville (1988) who caution against the conversion from one to the other using empirical formulae that are known to be erroneous. Therefore, we do not convert MMI values for other earthquakes (see previous sections) to EMS-98 intensity. Gahalaut et al. (2016) remark on the potential drawbacks and biases from inappropriate reinterpretation of "traditional" contoured isoseismal

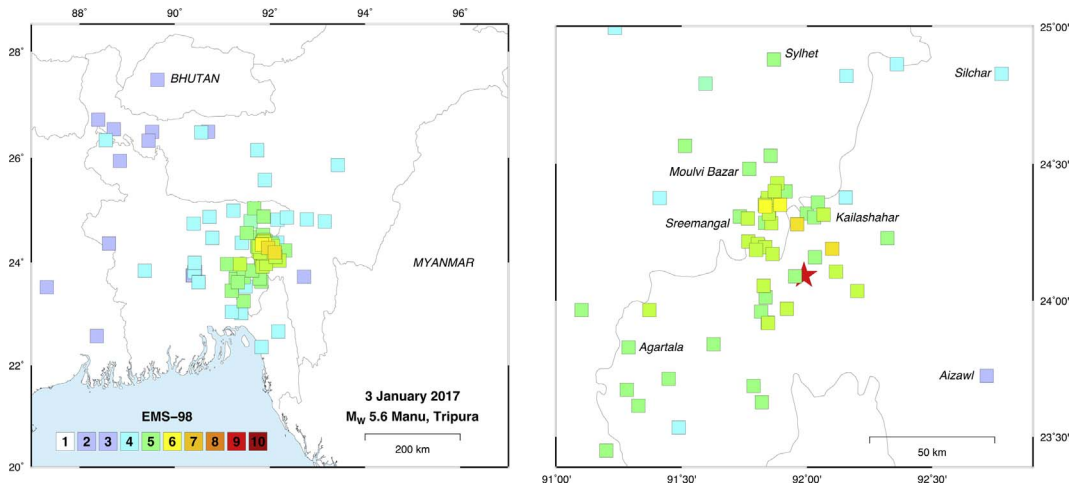

Fig. 3. Macroseismic observations and intensity assessments. Filled coloured squares represent locations where the 2017 Manu, Tripura earthquake was reported felt.

maps. In keeping with this we present raw point data (Fig. 3; Table S1) instead for the 2017 Manu earthquake. Each of our intensity data points are assigned a quality weighting scheme described by Musson (1998), to address uncertainties in the reliability of the numeric EMS-98 intensity assignment, the resolution of geo-spatial co-ordinates, the truthfulness of the available accounts or a combination of all or some of the above.

The 2017 Manu earthquake damaged at least 6727 structures in Tripura including 2154 and 4397 structures in Dhalai and Unakoti districts respectively (*Tripura State Disaster Management Authority report*, 9 January 2017). Based on our field survey and from reports in the local press, the highest intensity was 6–7 EMS at Jamtaibari and Shantipur where many mud houses (Type A buildings) suffered Grade 2 or worse damage (Table S1). Elsewhere in Tripura the earthquake was felt by most people, with minor damage (Grade 1) being reported from places such as Agartala. Beyond Tripura, the earthquake was strongly felt at Guwahati, Shillong and Silchar but was only lightly further to the west by the occupants of multi-storied buildings in Kolkata. In adjacent parts of Maulvi Bazar district in Bangladesh, singular house (6 EMS) or wall collapses (5–6 EMS) were reported from villages in the northern Dhalai (*also Doloi*) valley. Minor damage such as cracks (Grade 1) was reported from Chhatak, Moulvibazar, Nabiganj, Netrakona, Sreemangal and Sylhet, and also as far as Comilla. The earthquake was strongly felt in eastern and central parts of Bangladesh including at Chittagong and Dhaka but only mildly in western towns such as Rajshahi. Seismic seiches were observed in standing water at Narayanganj and Netrokona (*Daily Janakatha*, 4 January 2017).

5. Liquefaction

A striking feature of this earthquake was the occurrence of liquefaction in the epicentral region in Tripura (Fig. 4) and in the adjacent part of Bangladesh. Within India, sand blows and lateral spreads were observed on gentle slopes (< 5%) in agricultural land or along the Manu river near Kanchanbari (24.120°N, 91.994°E) in Tripura (Fig. 5). Eyewitnesses reported jets of water and sand spouting from these cracks, and from isolated sand blows on the banks of the Manu river. The length of these cracks ranged from ≈3 to ≈5 m (striking largely in a north–south direction). In Bangladesh, liquefaction occurred at several locations along the banks of the Dhalai river extending from the town of Kamalganj (24.35°N, 91.84°E) southward up to the border with India. Within the town of Kamalganj itself, sand and water was emitted from cracks in the Upazila playground (24.35119°N, 91.8461°E), and south of the town liquefaction was confined to an abandoned meander that was clearly discernible from satellite imagery (24.3567°N, 91.8481°E). Press reports (*Uttar Purbo*, 4 January 2017) also alleged cracks formed on the banks of the Barak river near Nabiganj (24.566°N, 91.513°E) at a distance of ≈70 km but we were unable to independently confirm this information. Unfortunately, it was unknown to us whether these liquefaction features developed co- or post-seismically. However, at one location i.e. Ramnagar (24.11°N, 91.98°E) in Unakoti, an eyewitness recalled water flowing out of cracks for up to 5-min following the cessation of shaking (Malay Kumar Deb, https://www.youtube.com/watch?v=AwDujYwwLk0).

Ambraseys (1988) and Castilla and Audemard (2007) used recorded liquefaction from global earthquakes to establish a relationship between moment magnitude and the farthest distance (R_E) at which liquefaction was observed. Similar relationships have been derived using regional datasets, for example in New Zealand (Maurer et al., 2015), or for R_E with respect to surface-wave magnitudes (Galli, 2000). Seismically assisted liquefaction or associated ground failure is not uncommon in eastern Bangladesh and adjacent parts of India with noteworthy occurrences caused by significant earthquakes in 1548, 1596, 1697 (Iyengar et al., 1999), 1846, 1865 (Martin and Szeliga, 2010), 1869 (Oldham, 1883b), 1880 (Gahalaut et al., 2016), 1897 (Oldham, 1899), 1918 (Stuart, 1920), 1947 (Martin and Szeliga, 2010), 1950 (Poddar, 1953), 1984 (Agrawal, 1986), 1988 (Gupta, 1993) and 2016 (Gahalaut et al., 2016). An earthquake on 14 October 1882 was felt as far as Darjeeling and Kolkata (Indian Daily News, 14 October 1882) and was responsible for the destruction of a pucca house at Burnie Braes (Indian Mirror, 29 October 1882). During this earthquake, cracks formed in the ground at Silchar from which "a good deal of water" was emitted (*Englishman*, 14 October 1882; *Indian Daily News*, 16 October 1882). When our field observations or the reports of liquefaction available to us from the 2017 Manu earthquake, are compared (Fig. 6) to predicted curves (Ambraseys, 1988; Galli, 2000; Castilla and Audemard, 2007), the observations from India fall within the expected range but the reports from Bangladesh at $R_E > 10$ km stand out as outliers.

6. Discussion

The depth of the gently dipping décollement between the overlying Indo-Burmese wedge and the underlying Indian plate ranges between 25 and 30 km in the Tripura region (Steckler et al., 2008; Kundu and Gahalaut, 2012; Russo, 2012). The relatively deeper focal depth, and the inferred motion on a vertical plane implicate a source within the underlying Indian slab, similar to the 2016 Tamenglong, Manipur earthquake (Gahalaut and Kundu, 2016; Gahalaut et al., 2016) and several other earthquakes in the region (Rao and Kalpna, 2005; Kundu and Gahalaut, 2012; Russo, 2012). Our preliminary analysis of the data is unable to identify the fault plane from the two nodal planes but we prefer the NNW oriented nodal plane to be the fault plane based on the

Fig. 4. Observations of soil liquefaction and sand blows (24.1202°N and 91.9926°E).

Fig. 5. Lateral spread, mostly slope failure, in an agricultural field (24.1202°N and 91.9941°E).

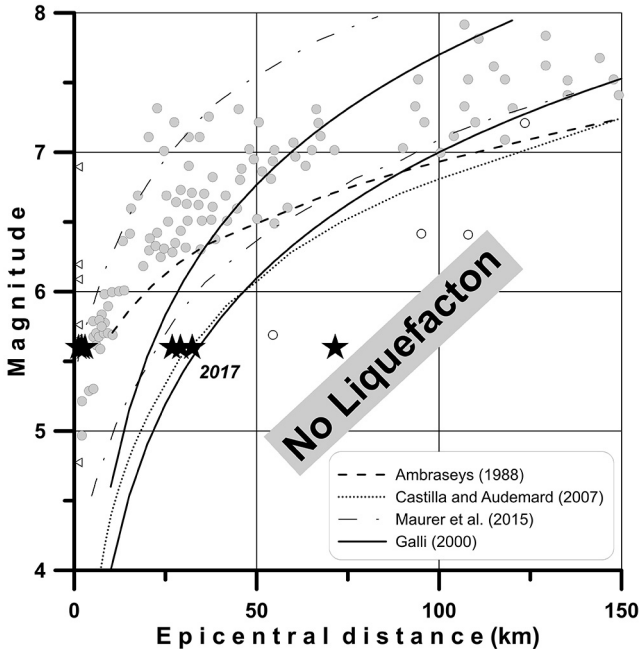

Fig. 6. Various empirical relations between the maximum distal liquefaction and earthquake magnitude. Filled and open circles are the worldwide data used by Ambraseys (1988) for shallow and deep earthquakes. Two dashed-dotted curves define the 7% (lower curve) and 93% (upper curve) liquefaction probabilities estimated by Maurer et al. (2015). Stars indicate liquefaction caused by the 2017 earthquake in the Manu region in India and in the Kamalganj area in Bangladesh.

observed damage patterns. The strike of this plane is similar to the fault plane identified for the 2016 Tamenglong earthquake (Parameswaran and Rajendran, 2016; Singh et al., 2016). Stork et al. (2008) and Russo (2012) identified slab contortion and segmentation, and possible tears in the Indian lithospheric slab under the wedge from offsets in intermediate depth earthquakes, and anisotropy in the upper mantle. Overall, all these earthquakes are consistent with the Indian lithospheric slab sinking, while also being subjected to along strike compression and bending below this arc (Russo, 2012). As noted previously, interpretations of geodetic data from India, Bangladesh, and Myanmar are not unanimous in the seismic hazard potential of the décollement under the outer wedge (Gahalaut et al., 2013; Steckler et al., 2016). Our source parameters determined for the Manu earthquake based on instrumental observations indicate that this earthquake occurred beneath the outer wedge identified by Steckler et al. (2016) but not on the interface between the overriding wedge and the underlying Indian slab.

Irrespective of whether a megathrust earthquake can occur in this region, the Manu earthquake emphasises the hazard posed by the occurrence of moderate to large intra-slab earthquakes in the region. Such earthquakes in close proximity to the heavily populated Bengal basin. This region is known to have the potential to locally amplify ground motions in unconsolidated or reworked deltaic sediments (e.g. Islam et al., 2010; Asad et al., 2015; Khan, 2016), and together with a poor record when it comes to rigorously implementing building regulations (e.g. Sabet and Tazreen, 2015), can have serious societal and economic consequences in larger future earthquakes. Although intraslab earthquakes are not frequently as deadly or as damaging as their shallow counterparts, experiences from Indonesia (e.g. Sengara et al., 2010), Mexico (e.g. Meehan, 1974; Singh et al., 1999), Pakistan (e.g. Coulson, 1938) and eastern Europe (e.g. Mândrescu and Radulian, 1999; Konrod et al., 2013) serve as counter-examples.

As in the 2016 Tamenglong, Manipur earthquake (Gahalaut et al., 2016), the peak ground acceleration (PGA) recorded at Shillong (SHL) during the Manu earthquake at a distance of 172 km from the epicentre

was higher than expected (Table 2), and was in fact higher than at an instrument located 100 km from the epicentre at Belonia in Tripura. Interestingly, for Shillong the conversion of the instrumented PGA to macroseismic intensity showed good correspondence with the actual observed macroseismic intensity. The instrument at Shillong is located at an elevation of 1600 m and is situated on quartzite ridge belonging to the Precambrian Shillong group corresponding to an NEHRP site A classification (Mittal et al., 2012). Once again, as was the case with the 2016 Tamenglong, Manipur earthquake (Gahalaut et al., 2016), we suspect this instrumental observation represents topographic amplification that produced aggravated strong motion when coupled with or without soil amplification as has been observed elsewhere (e.g. Buchon and Barker, 1996; Hough et al., 2010; Assimaki et al., 2005; Nagashima et al., 2012; Assimaki and Joeng, 2013), and that this instrumental observation was possibly further aggravated by along strike directivity as observed by Benetatos and Kiratzi (2004) in eastern Europe. However, given that our inference relies upon observations from a meagre sample of two earthquakes alone, we caution against assuming this to be the norm. Although beyond the scope of this study, a through reanalysis of other strong motion records from Shillong might shed further insights. Nonetheless, it might be worthy to remind the reader of the extreme vertical accelerations documented during the 12 June 1897 Shillong earthquake. The projection, displacement, or snapping of monoliths in the Khasi and Jaintia Hills (Oldham, 1899; Ambraseys and Bilham, 2003; Bilham, 2008), and the observation of stones thrown into the air like "*like peas on a drum*" in Shillong (Oldham, 1899), could have plausibly also been the result of amplified local site effects rather than free field surface ground motions.

The liquefaction from the 2017 Manu earthquake was spatially restricted to the Manu and Dhalai river valleys in Tripura and Bangladesh respectively. In comparison with empirical curves that relate magnitudes of shallow earthquakes (< 50 km) to the farthest expected occurrence of liquefaction features (Ambraseys, 1988; Castilla and Audemard, 2007), the liquefaction observations in the Dhalai valley in Bangladesh appear anomalous (Fig. 6). We were unable to confirm a report of cracks on the banks of the Barak river in Nabiganj upazila. Globally, examples of liquefaction at anomalously large distances exist in published literature (e.g. Papadopoulos, 1993; Rajendran et al., 2002; Hozler et al., 2005). The Dhalai valley is a synclinal feature, and downstream within Bangladesh the youngest sedimentary facies are of Quaternary age consisting of unconsolidated light grey clay, silt, and fine to coarse, grey and yellow grained sand (Rahman, 1979). In Tripura, these overlay the Pliocene to early Quaternary Duptila formation, consisting of loose, unconsolidated ferruginous sandstone with pink and yellow clay bands (Kesari, 2011), that extends along the Dhalai valley up to the Bangladesh border. The Dhalai valley is bounded on either side by outcrops of older lithologies i.e. the Tipam and Surma groups that outcrop as the Atharamura and Bhatchia anticlines in Tripura, to the west and the east respectively, within an approximately north–-south striking fold and thrust belt (Ganguly, 1993). Lithologically similar formations exist in the Manu valley bounded by the Bhatchia anticline to the west, and the Harargaj, and Machlithum anticlines to the east (Ganguly, 1993). In particular, north of Kanchanpur the valley floor consists of Holocene alluvium with a clay content associated or intermixed with sands and silts (Kesari, 2011). Ground failure susceptibility is a function of topography and the properties of the unit such as its sedimentation process, the age of deposition, geological history, depth of the water table, grain size distribution, density state, depth of burial, ground slope, and proximity to a free face (Youd and Perkins, 1978). Liquefaction features for the 2017 Manu earthquake were reported from villages within the flood plain of the Dhalai river. A field visit to the site south of Kamalganj and a review of satellite imagery of the same indicates liquefaction in this area was concentrated in an abandoned meander of unknown age. Holocene flood plain deposits are highly susceptible to liquefaction, with very loosely compacted sand and recently deposited river channel sediments prone to liquefaction at larger than expected distances (Youd and Perkins, 1978). Furthermore, directivity in energy radiation from the source is an important contributing factor (Audemard et al., 2005; Castilla and Audemard, 2007) as well the role of local attenuation (Youd and Perkins, 1978), or the amplification (or damping) of ground motions. Other than at Agartala, no strong motions instruments were present within the epicentral region in Tripura but the distribution of macroseismic intensities appear to suggest directivity towards the north–north-west. Incidentally, locations with liquefaction in the Dhalai valley in Bangladesh are at an azimuth of $\approx 340^{o}$ in other words, within 10° of the strike of one of the nodal plane of the 2017 Manu earthquake (Table 1). Both Ambraseys (1988) and Castilla and Audemard (2007) use point source models, i.e. they consider epicentral distance (R_E) and not rupture distance in their regression analysis, and the uncertainty associated with these liquefactions curves is unreported. Nevertheless, even when we assumed an empirically determined subsurface rupture length (Wells and Coppersmith, 1994) of ≈ 8 km for the 2017 Manu earthquake, with south to north directivity, the locations in Bangladesh appear as distinct outliers with respect to Ambraseys (1988) while straddling the Castilla and Audemard (2007) curve. At this preliminary stage, we therefore conclude that the liquefaction features observed in the Dhalai valley in Bangladesh were most likely anomalous and that they were controlled by local site conditions and possibly by rupture directivity.

In response to the shaking caused by the passage of seismic waves through loosely packed cohesionless sediments, there is an increase in pore-water pressure caused by the amplitude of the cyclic shear stress, and the number of applications of this stress in turn depend on the peak acceleration and duration of strong shaking (Seed, 1979; McCalpin, 1996). Depending upon the depth of the liquefied sandy layer, the liquefied material might have spouted with some delay with respect to the different phases of the earthquake waveform (P, S or surface waves). However, since there is no information on the exact time of occurrence of soil liquefaction and the depth of the liquefied layer at each of the sites we list, it is not possible to comment on which seismic phase was responsible for the observed liquefaction.

Liquefaction has occurred on several occasions in the region of the Indo-Burmese wedge as noted in previous sections. Despite having had an intermediate focus (~ 90 km), the M_W 7.2 Indo-Myanmar earthquake on 6 August 1988 located 120 km east-northeast of Imphal produced liquefaction at several places in Assam (Gupta, 1993). However, the severest and most extensive liquefaction in this immediate region occurred during the M_I 7.1–7.4 Cachar earthquake in 1869 (Ambraseys and Douglas, 2004; Gahalaut et al., 2016) that included lateral spreads and slumping along the Barak river in the Silchar region, and sand vented from fissures in the Manipur Valley (Oldham, 1883a). It has been proposed that the sediments of the Indo-Burmese wedge are overpressured (Steckler et al., 2008). Whether or not this implies that these sediments are more prone to liquefaction is a matter of debate. The processes controlling the occurrences of relatively deeper rooted mud-volcanoes at some places in the Indo-Burmese wedge (Steckler et al., 2008) could be related with the over-pressured wedge. It should be noted here that in all previous cases of liquefaction, regions closest to river channels or paleochannels were most susceptible. Furthermore, liquefaction commonly originates at depths of 10 m in saturated sediments (McCalpin, 1996). Therefore, we make the inference that liquefaction observed thus far in the Indo-Burmese wedge has been controlled by local rather than regional conditions. In the case of the Manu earthquake the observed liquefaction features may have also been confined to the shallow subsurface and were therefore unrelated or unconnected to conditions at depth.

7. Conclusions

The 2017 Manu earthquake is one of the largest instrumentally recorded earthquakes in the state of Tripura in India, and is only overshadowed in the immediate region by the 1918 Sreemangal earthquake.

The focal depth of 31 km, and slip inferred to have occurred on a vertical plane, imply an intraslab origin for this earthquake i.e. that it occurred within the Indian plate underlying the Indo-Burmese wedge. Damage from the 2017 earthquake was limited to un-engineered structures within the epicentral region but minor non-structural damage also occurred in adjacent parts of Bangladesh. As in Gahalaut et al. (2016), we once again suggest the role of topographic amplification in strong motion observations from Shillong in India but underscore the need for further investigation of these. Despite the low magnitude of the Manu earthquake, liquefaction that included sand blows and lateral spreads were observed within the epicentral region and at anomalously large distances in Bangladesh. The incidence of such features underscores the hazard posed by the presence of unconsolidated saturated sediments beneath the densely population Bengal basin region that pose a major threat to life and property as they may exacerbate damage during future, large intraslab or interface rupturing earthquakes.

Acknowledgments

We thank NCS personnel who are responsible for the installation and maintenance of seismological observatories, and for their involvement in earthquake monitoring in India. Chandan Kumar Thakur and Khasuram Reang assisted in the field. This article benefitted from useful discussions with Aurélie Coudurier-Curveur, Çağıl Karakaş, Rahul Bhattacharya, and three anonymous reviewers. SSM was supported by Kerry Sieh through the National Research Foundation, Singapore, and the Singapore Ministry of Education under the Research Centres of Excellence initiative. AA was supported by the Geological Survey of Bangladesh. The field survey in India was financially supported by the Ministry of Earth Sciences (MoES/P.O.(Seismo)/1(257)/2015). Figures were prepared using the freely available Generic Mapping Tools (GMT) software (Wessel and Smith, 1999). The seismic data used in the study can be obtained from the corresponding author. This is Earth Observatory of Singapore contribution number 150.

Appendix A. Supplementary material

Supplementary data associated with this article can be found, in the online version, at http://dx.doi.org/10.1016/j.jseaes.2017.08.030.

References

Agrawal, P.N., 1986. Ground failure during the December 31, 1984, Cachar earthquake, northeast India. In: Proceedings of the 8th Symposium on Earthquake Engineering. University of Roorkee, pp. 159–166.

Ahsan, A., Kali, E., Coudurier Curveur, A., van der Woerd, J., Tapponnier, P., Alam, A.K., Ildefonso, Banerjee, S.P., Dorbath, C., 2015. Active faulting in Raghunandan Anticline, NE Bengal Basin, implications for future earthquake hazards. In: American Geophysical Union, Fall Meeting 2015, abstract #T41B-2885.

Allmann, B., Shearer, P., 2009. Global variations of stress drop for moderate to large earthquakes. J. Geophys. Res. 114, B01310. http://dx.doi.org/10.1029/2008JB00582.

Ambraseys, N.N., 1988. Engineering seismology: Part 2. Earthquake Eng. Struct. Dynam. 17, 1–105. http://dx.doi.org/10.1002/eqe.4290170102.

Ambraseys, N., Bilham, R., 2003. Reevaluated intensities for the great Assam Earthquake of 12 June 1897, Shillong, India. Bull. Seismol. Soc. Am. 93, 655–673. http://dx.doi.org/10.1785/0120020093.

Ambraseys, N.N., Douglas, J., 2004. Magnitude calibration of north Indian earthquakes. Geophys. J. Int. 159, 165–206. http://dx.doi.org/10.1111/j.1365-246X.2004.02323.x.

Ambraseys, N.N., Melville, C.P., 1988. An analysis of the eastern Mediterranean earthquake of 20 May 1202. In: Historical Seismograms and Earthquakes of the World. Academic Press, San Diego, California, pp. 181–200.

Anonymous, 1919. Report on the administration of Assam: 1918–1919. Assam Secretariat Printing Office, Shillong, pp. 52–53.

Anonymous, 1920. Annual Report of the Archaeological Survey of India: Eastern Circle. Government Printing, Bihar & Orissa, pp. 3–4.

Asad, M.A., Islam, S., Siddique, M.N.A., 2015. Effect of high peak ground acceleration on the liquefaction behaviour of subsoil and impact on the environment. J. Civ. Eng. Res. 5 (4), 83–89. http://dx.doi.org/10.5923/j.jce.20150504.02.

Assimaki, D., Gazetas, G., Kausel, E., 2005. Effects of local soil conditions and topographic aggravation of seismic motion: parametric investigation and recorded field evidence from the 1999 Athens earthquakes. Bull. Seismol. Soc. Am. 95, 1059–1089.

Assimaki, D., Joeng, S., 2013. Ground motion observations at Hotel Montana during the M7.0 2010 Haiti earthquake: topography or soil amplification? Bull. Seismol. Soc. Am. 103, 2577–2590.

Atkinson, G.M., 2007. Relationships between felt intensity and instrumental ground motion in the Central United States and California. Bull. Seismol. Soc. Am. 97 (2), 497–510. http://dx.doi.org/10.1785/0120060154.

Audemard, F.A., Gomez, J.C., Tavera, H.J., Orihuela, G.N., 2005. Soil liquefaction during the Arequipa M_W 8.4, June 23, 2001, earthquake, southern coastal Peru. Eng. Geol. 78, 237–255.

Benetatos, C.A., Kiratzi, A.A., 2004. Stochastic strong ground motion simulation of intermediate depth earthquakes: the cases of the 30 May 1990 Vrancea (Romania) and of the 22 January 2002 Karpathos island (Greece) earthquakes. Soil Dyn. Earthq. Eng. 24 (1), 1–9. http://dx.doi.org/10.1016/j.soildyn.2003.10.003.

Bilham, R., 2008. Tom La Touche and the Great Assam Earthquake of 12 June 1897: letters from the epicenter. Seismol. Res. Lett. 79 (3), 426–437. http://dx.doi.org/10.1785/gssrl.79.3.426.

Brune, J., 1970. Tectonic stress and the spectra of seismic shear waves from earthquakes. J. Geophys. Res. 75, 4997–5009.

Buchon, M., Barker, J.S., 1996. Seismic response of a hill: the example of Tarzana, California. Bull. Seismol. Soc. Am. 86, 66–72.

Castilla, R.A., Audemard, F.A., 2007. Sand blows as a potential tool for magnitude estimation of pre-instrumental earthquakes. J. Seismolog. 11, 473–487.

Chen, W.-P., Molnar, P., 1990. Source parameters of earthquakes and intraplate deformation beneath the Shillong Plateau and the northern Indoburman ranges. J. Geophys. Res. 95 (B8), 12527–12552.

Coulson, A.L., 1938. Hindukush earthquake of the 14th November 1937. Rec. Geol. Surv. India 73 (1), 135–141.

Dixit, A.M., Ringler, A., Sumy, D., Cochran, E., Hough, S.E., Martin, S.S., Gibbons, S., Luetgert, J., Galetzka, J., Shrestha, S.N., Rajaure, S., McNamara, D., 2015. Strong motion recordings of the M7.8 Gorkha, Nepal, earthquake sequence from low-cost, Quake Catcher Network accelerometers. Seismol. Res. Lett. 86 (6), 1533–1539. http://dx.doi.org/10.1785/0220150146.

Du, W., Goh, K.S., Pan, T.-C., 2016. Methodology for estimating human response to tremors in high-rise buildings. J. Seismolog. http://dx.doi.org/10.1007/s10950-016-9628-y.

Gahalaut, V.K., Kundu, B., 2016. The 4 January 2016 Manipur earthquake in the Indo-Burmese wedge, an intra-slab event. Geomat. Nat. Haz. Risk 7, 1506–1512. http://dx.doi.org/10.1080/19475705.2016.1179686.

Gahalaut, V.K., Kundu, B., Laishram, S.S., Catherine, J., Kumar, A., Devchandra, M., Tiwari, R.P., Samanta, S.K., Ambikapathy, A., Mahesh, P., Bansal, Amit., Narsaiah, M., 2013. Aseismic plate boundary in the Indo-Burmese wedge, northwest Sunda Arc. Geology 41, 235–238.

Gahalaut, V.K., Martin, S.S., Srinagesh, D., Kapil, S.L., Suresh, G., Saikia, S., Kumar, V., Dadhich, H., Patel, A., Prajapati, S.K., Shukla, H.P., Gautam, J.L., Baidya, P.R., Mandal, S., Jain, A., 2016. Seismological, geodetic, macroseismic and historical context of the 2016 M_W 6.7 Tamenglong (Manipur) India earthquake. Tectonophysics 688, 36–48. http://dx.doi.org/10.1016/j.tecto.2016.09.017.

Galli, P., 2000. New empirical relationships between magnitude and distance for liquefaction. Tectonophysics 324, 169–187.

Ganguly, S., 1993. Stratigraphy, sedimentation and hydrocarbon prospects of the tertiary succession of Tripura and Cachar (Assam). Indian J. Geol. 65, 145–180.

Grünthal, G., 1998. The European Macroseismic Scale EMS-98, 15. Conseil de l'Europe, Cahiers du Centre Europeén de Geodynamique et de Seismoligie, Luxembourg, pp. 101.

Gupta, M.K., 1993. Liquefaction During 1988 Earthquakes and a Case Study, Proceedings: Third International Conference on Case Histories in Geotechnical Engineering, St. Louis, Missouri, June 1–4, 1993, Paper No. 14.19, pp. 1757–1761.

Guzman-Speciale, M., Ni, J.F., 1996. Seismicity and active tectonics of the Western Sunda Arc. In: Yin, A., Harrison, T.M. (Eds.), Tectonic Evolution of Asia. Cambridge University Press, pp. 63–84.

Guzman-Speziale, M., Bevis, M., Holt, W.E., Wallace, T.C., Seager, W.R., 1989. Accretionary tectonics of Burma and the three-dimensional geometry of the Burma subduction zone. Geology 17, 68–71.

Hough, S.E., Altidor, J.R., Anglade, D., Given, D., Janvier, M.G., Maharrey, J.Z., Meremonte, M.B., Mildor, S.-L., Prepetit, C., Yong, A., 2010. Localised damage caused by topographic amplification during the 2010 M7.0 Haiti earthquake. Nat. Geosci. 3, 778–782. http://dx.doi.org/10.1038/ngeo988.

Hough, S.E., Martin, S.S., Gahalaut, V.K., Joshi, A., Landès, M., Bossu, R., 2016. A comparison of observed and predicted ground motions from the 2015 M_W 7.8 Gorkha, Nepal, earthquake. Nat. Hazards 84 (3), 1661–1684.

Hozler, T.L., Noce, T.E., Bennett, M.J., Tinsley III, J.C., Rosenberg, L.I., 2005. Liquefaction at Oceano, California, during the 2003 San Simeon Earthquake. Bull. Seismol. Soc. Am. 95 (6), 2396–2411.

Hunter, W.W., Cotton, J.S., Burn, R., Meyer, W.S., 1909. The Imperial Gazetteer of India. Clarenden, Oxford, England.

Islam, M.S., Hossein, M.T., Ameen, S.F., Hoque, E., Ahamed, S., 2010. Earthquake induced liquefaction vulnerability of reclaimed areas in Dhaka. J. Civ. Eng. 38 (1), 65–80.

Iyengar, R.N., Sharma, D., Siddiqui, J.M., 1999. Earthquake history of India in medieval times. Indian J. Hist. Sci. 34 (3), 181–237.

Kesari, G.K., 2011. Geology and mineral resources of Manipur, Mizoram, Nagaland and Tripura, Geological Survey of India, Miscellaneous Publication, 30, IV, 1, (Part 2).

Khan, A.A., 2015. Geophysical characterization and earthquake hazard vulnerability of Dhaka Mega City, Bangladesh, vis-à-vis impact of scenario earthquakes. Nat. Hazards

82 (2), 1147–1166. http://dx.doi.org/10.1007/s11069-016-2237-9.
Konrod, T., Radulian, M., Panza, G., Popa, M., Paskaleva, I., Radovanovich, S., Gibovszki, K., Sandu, I., Pekevski, L., 2013. Integrated transnational macroseismic data set for the strongest earthquakes of Vrancea (Romania). Tectonophysics 590, 1–23.
Kundu, B., Gahalaut, V.K., 2012. Earthquake occurrence process in the Indo-Burmese wedge and Sagaing fault region. Tectonophysics 524, 135–146. http://dx.doi.org/10.1016/j.tecto.2011.12.031.
Le Dain, A.Y., Tapponnier, P., Molnar, P., 1984. Active faulting and tectonics of Burma and surrounding regions. J. Geophys. Res. 89, 453–472.
Mândrescu, N., Radulian, M., 1999. Macroseismic field of the Romanian intermediate depth earthquakes, in Vrancea Earthquakes: Tectonics, Hazard and Risk Mitigation. Adv. Natural Technol. Hazards Res. 11, 163–174.
Martin, S.S., Szeliga, W., 2010. A catalog of felt intensity data for 589 earthquakes in India, 1636–2008. Bull. Seismol. Soc. Am. 100 (2), 536–569. http://dx.doi.org/10.1785/0120080329.
Martin, S.S., Kakar, D.M., 2012. The 19 January 2011 M_W 7.2 Dalbandin earthquake, Balochistan. Bull. Seismol. Soc. Am. 100 (4), 1810–1819. http://dx.doi.org/10.1785/0120110221.
Martin, S.S., Hough, S.E., 2016. Reply to, “Comment on 'Ground Motions from the 2015 M_W 7.8 Gorkha, Nepal, Earthquake Constrained by a Detailed Assessment of Macroseismic Data' by Stacey Martin, Susan E. Hough and Charleen Hung“ by Andrea Tertulliani, Laura Graziani, Corrado Castellano, Alessandra Maramai, Antonio Rossi. Seismol. Res. Lett. 87, 4. http://dx.doi.org/10.1785/0220160061.
Martin, S.S., Hough, S.E., Hung, C., 2015. Ground motions from the 2015 M_W 7.8 Gorkha, Nepal, earthquake constrained by a detailed assessment of macroseismic data. Seismol. Res. Lett. 86 (6), 1524–1532. http://dx.doi.org/10.1785/0220150138.
Maurer, B.W., Green, R.A., Quigley, M.C., Bastin, S., 2015. Development of magnitude-bound relations for paleoliquefaction analyses: New Zealand case study. Eng. Geol. 197, 253–266.
Maurin, T., Rangin, C., 2009. Structure and kinematics of the Indo-Burmese Wedge: recent and fast growth of the outer wedge. Tectonics 28 (2), TC2010.
Maurin, T., Masson, F., Rangin, C., Than Min, U., Collard, P., 2010. First global positioning system results in northern Myanmar: Constant and localized slip rate along the Sagaing fault. Geology 38, 591–594.
McCalpin, J., 1996. Palaeoseismology. Academic Press, San Diego, pp. 588.
Meehan, J.F., 1974. Reconnaissance report of the Veracruz, Mexico earthquake of August 28, 1973. Bull. Seismol. Soc. Am. 64 (6), 2011–2025.
Mittal, H., Kumar, A., Ramhmachhuani, R., 2012. Indian national strong motion instrumentation network and site characterization of its stations. Int. J. Geosci. 3, 1151–1167.
Musson, R., 1998. Intensity assignments from historical earthquake data: issues of certainty and quality. Annali di Geofsica 41 (1), 79–91.
Musson, R.M.W., Grunthal, G., Stucchi, M., 2010. The comparison of macroseismic intensity scales. J. Seismol. 14, 413–428. http://dx.doi.org/10.1007/s10950-009-9172-0.
Nagashima, F., Kawase, H., Matsushima, S., Sanchez-Sesma, F.J., Hayakawa, T., Satoh, T., Oshima, M., 2012. Application of the H/V spectral ratios for earthquake ground motions and microtremors at K-NET sites in Tohoku region, Japan to delineate soil non-lineality during the 2011 Off the Pacific Coast of Tohoku earthquake. In: Proceedings of the International Symposium on Engineering Lessons learned from the 2011 Great East Japan Earthquake, Tokyo, Japan.
Oldham, R.D., 1899. Report on the Great Earthquake of 12th June 1897, Memoirs of the Geological Survey of India, 29, Government of India.
Oldham, T., 1883a. A catalogue of Indian earthquakes from the earliest time to the end of A.D. 1869. Memoirs Geol. Surv. India 29, 163–215.
Oldham, T., 1883b. The Cachar Earthquake of 10th January 1869”. Memoirs Geol. Surv. India 29, 1–98.
Oliver, J., Murphy, L., 1971. WWNSS: seismology's global network of observing stations. Science 174, 254–261.
Pacheco, J.F., Sykes, L.R., 1992. Seismic moment catalog of large shallow earthquakes, 1900–1989. Bull. Seismol. Soc. Am. 82, 1306–1349.
Papadopoulos, G.A., 1993. The 20 March 1993 South Aegean, Greece, earthquake (Ms = 5.3): possible anomalous effects. Terra Nova 5, 399–404.
Parameswaran, R.M., Rajendran, K., 2016. The 2016 M_W 6.7 Imphal earthquake in the Indo-Burman range: a case of continuing intraplate deformation within the subducted slab. Bull. Seismol. Soc. Am. 106, 6.
Prajapati, S.K., Dadhich, H.K., Chopra, S., 2017. Isoseismal map of the 2015 Nepal earthquake and its relationships with ground-motion parameters, distance and magnitude. J. Asian Earth Sci. 133, 24–37.
Poddar, M.C., 1953. A short note on the Assam Earthquake of 15th August, 1950, The Central Board of Geophysics, Publication No. 1, pp. 38–42.
Raghukanth, S.T.G., Somala, S.N., 2009. Modeling of strong-motion data in Northeastern India: Q, stress-drop and site amplification. Bull. Seismol. Soc. Am. 99 (2A), 705–725.
Rahman, Q.M.A., 1979. Geology of the southern part of Sylhet district Bangladesh. Rec. Geol. Surv. 2 (Part 2).
Rajendran, K., Rajendran, C.P., Thakkar, M., Gartia, R.K., 2002. Sand blows from the 2001 Bhuj earthquake reveal clues on past seismicity. Curr. Sci. 83 (5), 603–610.
Rao, N.P., Kalpna, 2005. Deformation of the subducted Indian lithospheric slab in the Burmese Arc. Geophys. Res. Lett. 32, L05301. http://dx.doi.org/10.1029/2004GL022034.
Rothé, J.P., 1969. The Seismicity of the Earth. UNESCO, Paris, pp. 336.
Russo, R.M., 2012. Source-side shear-wave splitting and upper-mantle flow beneath the Arakan slab, India-Asia-Sundalind triple junction. Geosphere 8, 158–178. http://dx.doi.org/10.1130/GES00534.1.
Sabet, D.M., Tazreen, A., 2015. Governing growth: understanding problems in real estate development in Dhaka, Bangladesh. J. S. Asian Dev. 10 (1), 1–21.
Seed, H.B., 1979. Soil liquefaction and cyclic mobility for level ground during earthquakes. J. Geotech. Eng., Am. Soc. Civ. Eng. 105, 201–255.
Sengara, I.W., Suarjana, M., Beetham, D., Corby, N., Edwards, M., Griffith, M., Wehner, M., Weller, R., 2010. The 30 September 2009 West Sumatra Earthquake: Padang Region Damage Survey. Geoscience Australia Publication, Camberra.
Singh, A.P., Purnachandra Rao, N., Ravi Kumar, M., Hsieh, M.-C., Zhao, L., 2016. Role of the Kopili fault in deformation tectonics of the Indo-Burmese arc inferred from the rupture process of the 3 January 2016 M_W 6.7 Imphal earthquake. Bull. Seismol. Soc. Am. 107. http://dx.doi.org/10.1785/0120160276.
Singh, S.K., Ordaz, M., Pacheco, J.F., Quaas, R., Alcántara, L., Alcocer, S., Gutirrez, C., Meli, R., Ovando, E., 1999. A preliminary report on the Tehuacán, Mexico earthquake of June 15, 1999 (M_W = 7.0). Seismol. Res. Lett. 70 (5), 489–504.
Socquet, A., Vigny, C., Chamot-Rooke, N., Simons, W., Rangin, C., Ambrosius, B., 2006. India and Sunda plates motion and deformation along their boundary in Myanmar determined by GPS. J. Geophys. Res. 111, B05406.
Sohoni, V.V., 1951. Seismological Bulletin – December 1950. Government of India: Meteorological Department, pp. 21–22.
Steckler, M.S., Akhter, S.H., Seeber, L., 2008. Collision of the Ganges-Brahmaputra Delta with the Burma Arc: implications for earthquake hazard. Earth Planet. Sci. Lett. 273 (3), 367–378.
Steckler, M.S., Mondal, D.R., Akhter, S.H., Seeber, L., Feng, L., Gale, J., Hill, E.M., Howe, M., 2016. Locked and loading megathrust linked to active subduction beneath the Indo-Burman Ranges. Nat. Geosci. http://dx.doi.org/10.1038/NGEO2760.
Storchak, D.A., Di Giacomo, D., Istvan, B., Engdahl, E.R., Harris, J., Lee, W.H.K., Villaseñor, A., Bormann, P., 2013. Public release of the ISC-GEM global instrumental earthquake catalogue (1900–2009). Seismol. Res. Lett. 84, 810–815.
Stork, A.L., Selby, N.D., Heyburn, R., Searle, M.P., 2008. Accurate relative earthquake hypocenters reveal structure of the Burma subduction zone. Bull. Seismol. Soc. Am. 98, 2815–2827.
Stuart, M., 1919. Preliminary note on the Srimangal earthquake of July 8th, 1918. Rec. Geol. Surv. 49 (3), 173–189.
Stuart, M., 1920. The Srimangal earthquake of 8th July 1918. Memoirs Geol. Surv. 46, 1–70.
Szeliga, W., Hough, S.E., Martin, S., Bilham, R., 2010. Intensity, magnitude, location, and attenuation in India for felt earthquakes since 1762. Bull. Seismol. Soc. Am. 100, 570–584. http://dx.doi.org/10.1785/0120080329.
Tandon, A.N., 1954. Study of the great Assam earthquake of August 1950 and its aftershocks. Indian J. Meteorol. Geophys. 5 (2), 95–137.
Tandon, A.N., 1963. Seismological notes: April–June 1963. Indian J. Meteorol. Geophys. 14, 514.
Triantafyllis, N., Sokos, E., Ilias, A., Zahradník, J., 2015. Scisola: automatic moment tensor solution for SeisComP3. Seismol. Res. Lett. 87, 157–163.
Van Noten, K., Lecocq, T., Sira, C., Hinzen, K.-G., Camelbeeck, T., 2016. Path and site effects deduced from transfrontier internet macroseismic data of two recent M4 earthquakes in NW Europe. Solid Earth Discuss. http://dx.doi.org/10.5194/se-2016-150.
Vigny, C., Socquet, A., Rangin, C., Chamot-Rooke, N., Pubellier, M., Bouin, M., Bertrand, G., Becker, M., 2003. Present-day crustal deformation around Sagaing fault, Myanmar. J. Geophys. Res. 108, 2533. http://dx.doi.org/10.1029/2002JB001999.
Wald, D.J., Quitoriano, V., Dengler, L., Dewey, J.W., 1999. Utilization of the internet for rapid community intensity maps. Seismol. Res. Lett. 70 (6), 680–697. http://dx.doi.org/10.1785/gssrl.70.6.680.
Wang, Y., Sieh, K., Tun, S.T., Lai, K.-Y., Myint, T., 2014. Active tectonics and earthquake potential of the Myanmar region. J. Geophys. Res. – Solid Earth 119, 3767–3822.
Wells, D.L., Coppersmith, K.J., 1994. New empirical relations among magnitude, rupture length, rupture width, rupture area and surface displacement. Bull. Seismol. Soc. Am. 84 (4), 974–1002.
Wessel, P., Smith, W.H.F., 1999. Free software helps map and display data. Eos Trans., AGU 72, 441–445. http://dx.doi.org/10.1029/90EO00319.
Worden, C.B., Gerstenberger, M.C., Rhoades, D.A., Wald, D.J., 2012. Probabilistic relationships between ground-motion parameters and modified Mercalli intensity in California. Bull. Seismol. Soc. Am. 102, 204–221. http://dx.doi.org/10.1785/0120110156.
Youd, T.L., Perkins, D.M., 1978. Mapping liquefaction-induced ground failure potential. J. Geotech. Eng. Div., ASCE 104 (GT4), 433–446.